https://www.cytojournal.com/

CytoJournal

Editor-in-Chief:
Miaoqing Zhao, PhD., MD (Shandong First Medical University, Jinan, China)
He Wang, MD, PhD (Yale University School of Medicine, New Haven, Connecticut, USA)
Founding Editor & Editor-in-chief Emeritus:
Vinod B. Shidham, MD, FIAC, FRCPath (WSU School of Medicine, Detroit, USA)

OPEN ACCESS

Research Article

A new perspective: Acyl-CoA synthetase long-chain family member 4 inhibits ubiquitin-specific protease 7-induced epithelial ovarian cancer progression by inducing ferroptosis and M1 macrophage polarization

Yazhou Qi, MM[1#], Qianwen Li, MM[1#], Limin Chen, BD[1], Shuimiao Zhao, MM[1], Jiaoran Nie, MM[2], Gaoyuan Liu, MM[1]*

[1]Department of Gynaecology, Affiliated Hospital of Hebei University, Baoding, [2]Department of Gynaecology, Zhangjiakou First Hospital, Zhangjiakou, Hebei, China.

[#]Yazhou Qi and Qianwen Li contributed equally to this article.

***Corresponding author:**

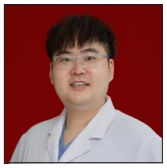

Gaoyuan Liu,
Department of Gynaecology,
Affiliated Hospital of Hebei University, Baoding, Hebei, China.

gaoyuanliu6@163.com

Received: 28 November 2024
Accepted: 15 January 2025
Published: 05 March 2025

DOI
10.25259/Cytojournal_241_2024

Quick Response Code:

ABSTRACT

Objective: Epithelial ovarian cancer (EOC) is the most common and lethal type of ovarian cancer, and the cross-talk between tumor cell ferroptosis and macrophages is essential to cancer progression. This study aims to investigate the roles of ubiquitin-specific protease 7 (USP7) and acyl-CoA synthetase long-chain family member 4 (ACSL4) in the pathogenesis of EOC.

Material and Methods: The expression patterns of USP7 and ACSL4 in EOC cell lines were first determined by quantitative reverse transcription polymerase chain reaction (qRT-PCR) and Western blot. ACSL4 recombinant protein was applied alone or in conjunction with a USP7 overexpression plasmid in EOC cells, and the effects of USP7 and ACSL4 on EOC cell proliferation and apoptosis were assessed using colony formation assays and terminal deoxynucleotidyl transferase deoxyuridine triphosphate (dUTP) nick end labeling staining. The effects of USP7 and ACSL4 on ferroptosis in EOC cells were evaluated by measuring reactive oxygen species (ROS) fluorescence intensity, malondialdehyde (MDA), glutathione (GSH) levels, and glutathione peroxidase 4 (GPX4) messenger RNA (mRNA) levels. Co-culture of EOC cell-conditioned medium treated with ACSL4 recombinant protein or USP7 overexpression plasmid was performed with Human Acute Monocytic Leukemia Cell Line (THP-1) macrophages, and the expression levels of cluster of differentiation 86 and cluster of differentiation 206 were analyzed by flow cytometry. The expression levels of M1 polarization markers and M2 markers in macrophages were measured by qRT-PCR.

Results: ACSL4 was expressed at low levels in the EOC cell lines, whereas USP7 was expressed at high levels. Treatment with ACSL4 recombinant protein reduced colony formation and increased apoptotic cell levels in the EOC cells ($P < 0.001$). In addition, ACSL4 treatment increased ROS fluorescence intensity and MDA levels while decreasing GSH levels and GPX4 expression ($P < 0.001$). Furthermore, ACSL4 treatment promoted the polarization of THP-1 macrophages toward M1, increasing the expression of M1 markers ($P < 0.001$). USP7 overexpression exerted the opposite effect ($P < 0.001$).

Conclusion: This study reveals the critical role of USP7 in the progression of EOC. ACSL4 inhibits EOC growth and anti-apoptosis by inhibiting USP7-induced antiferroptosis and anti-M1 macrophage polarization, highlighting this mechanism as a potential therapeutic target in EOC.

Keywords: Acyl-CoA synthetase long-chain family member 4, Epithelial ovarian cancer, Ferroptosis, Macrophage, Ubiquitin-specific protease 7

INTRODUCTION

Epithelial ovarian cancer (EOC) is one of the deadliest gynecological malignancies worldwide, and its high mortality rate is primarily due to late-stage diagnosis, treatment resistance, and complex tumor microenvironment.[1,2] Understanding of the molecular mechanisms underlying EOC has progressed, and the roles of iron-dependent cell death (ferroptosis) and immune regulation in tumor progression represent emerging subjects of interest that can pave the way for novel therapeutic strategies.[3,4] A key regulator of ferroptosis, acyl-CoA synthetase long-chain family member 4 (ACSL4), is an enzyme that plays a crucial role in the synthesis of polyunsaturated fatty acids (PUFAs), which are particularly susceptible to peroxidation reactions.[5,6] ACSL4 promotes ferroptosis in various cancers by enhancing lipid peroxidation and oxidative stress, positioning it as a pivotal player in the non-apoptotic cell death pathway.[7-9]

Although ferroptosis has been extensively studied in various types of cancer, such as breast and liver cancer, its role in EOC has not been thoroughly explored. In addition, the relationship between ferroptosis and tumor immune microenvironment, particularly the polarization of tumor-associated macrophages (TAMs), is receiving increasing attention.[10-12] TAMs primarily exhibit two phenotypes: M1 macrophages, which possess pro-inflammatory and antitumor properties, and M2 macrophages, which support tumor growth and metastasis.[13] The interplay between ferroptosis and macrophage polarization remains poorly understood, especially in EOC, where the immune microenvironment plays a critical role in tumor progression.

Meanwhile, ubiquitin-specific protease 7 (USP7) has garnered significant attention as a key regulator of cellular processes in cancer due to its roles in deoxyribonucleic acid (DNA) repair, apoptosis, and immune evasion.[14,15] USP7 stabilizes critical oncogenic proteins, such as p53 and murine double minute 2 (MDM2), through its deubiquitinating activity, thereby promoting tumor progression.[16,17] However, the potential interplay between USP7 and ACSL4 in the regulation of ferroptosis and macrophage polarization has yet to be explored. Given the crucial role of ACSL4 in ferroptosis and the importance of USP7 in tumor immunity and survival, their interaction may represent a novel axis in the pathogenesis of EOC.

This study aims to investigate how USP7 influences ACSL4-mediated ferroptosis and the immune microenvironment, particularly focusing on the polarization of TAMs in EOC. We hypothesize that USP7 may promote the progression of EOC by counteracting the ferroptosis-inducing and M1 macrophage-polarizing effects of ACSL4. By revealing the molecular mechanisms underlying this interaction, we hope to identify novel therapeutic targets for the management of EOC and provide fresh insights into the role of ferroptosis and immune regulation in cancer treatment.

MATERIAL AND METHODS

Cell culture

The EOC cell line SKOV-3 (HTB-77) was purchased from the American Type Culture Collection (ATCC) (Manassas, Maryland, USA). The ovarian epithelial cells IOSE-80 (iCell-h112) and human monocytic leukemia cells THP-1 (iCell-h213) were purchased from Cellverse Co., Ltd. (Shanghai, China). All cells were cultured in their respective specialized media. THP-1 cells were stimulated with 150 nM phorbol-12-myristate-13-acetate (HY-18739, MedChemExpress, Monmouth Junction, New Jersey, USA) for 24 h to induce differentiation into macrophages. Subsequently, the conditioned medium (CM) from SKOV-3 cells was added to the THP-1-derived macrophages. The cells used in this study were verified through STR analysis and were confirmed to be free of mycoplasma contamination.

Cell treatment

SKOV-3 cells were treated with 10 μM ACSL4 recombinant protein (R10442h, EIAab, Wuhan, China) for 24 h. According to the manufacturer's instructions, the USP7 overexpression plasmid or negative control plasmid was transfected into SKOV-3 cells with a Lipofectamine 3000 reagent (L3000001, Thermo Fisher Scientific, Waltham, Massachusetts, USA) and designated as the Ov-USP7 and Ov-NC groups, respectively. SKOV-3 cells transfected with Ov-USP7 were exposed to ACSL4 recombinant protein (10 μM) and referred to as the Ov-USP7+ACSL4 group. The CM from SKOV-3 cells treated with Ov-USP7 and Ov-USP7+ACSL4 was added to the THP-1-derived macrophages.

Quantitative reverse transcription polymerase chain reaction (qRT-PCR)

First, total RNA was extracted from the cells with an RNA extraction kit (R0017S, Beyotime, Shanghai, China), and its purity and concentration were measured using NanoDrop (2000, Thermo Fisher Scientific, Waltham, Massachusetts, USA). Genomic DNA contamination was prevented by treating the extracted RNA with DNase I (18047019, Invitrogen, Carlsbad, California, USA), and then, reverse transcription reagents (D7168S, Beyotime, Shanghai, China) were used for synthesizing cDNA from RNA. Reverse transcription reaction is typically carried out at 42°C for 30 min, followed by termination at 85°C. Next, the qRT-PCR reaction system was prepared, including the cDNA template, forward and reverse primers for the target gene, SYBR Green reagent, buffer, and Taq DNA polymerase (D7207, Beyotime, Shanghai, China). The reaction program was set at 95°C for

5 min for initial denaturation, followed by 40 cycles of 95°C denaturation, 55°C annealing, and 72°C extension. After each extension step, fluorescence signals were detected. Finally, melt curve analysis was performed to confirm the specificity of the product. Data analysis was based on cycle threshold (CT) values for relative quantification. The $2^{-\Delta\Delta CT}$ method was used in calculating the relative expression of each gene, and β-actin served as the reference gene for normalizing target gene expression. Primer sequences are shown in Table 1.

Western blot

First, the protein was extracted from the cells with radioimmunoprecipitation assay (RIPA) buffer (P0013C, Beyotime, Shanghai, China), and protein concentration was measured using the bicinchoninic acid assay method (P0009, Beyotime, Shanghai, China). Next, the proteins were separated through sodium dodecyl sulfate polyacrylamide gel electrophoresis. Denatured protein samples were loaded onto polyacrylamide gels, and proteins were separated according to molecular weight through electrophoresis. Then, the separated proteins were transferred to a polyvinylidene fluoride membrane (FFP19, Beyotime, Shanghai, China), which was then blocked with 5% bovine serum albumin (P0007, Beyotime, Shanghai, China) before the transfer. Next, specific primary antibodies (ACSL4 (1:1000, ab205199, Abcam, Cambridge, UK) and β-actin (1:1000, ab8226, Abcam, Cambridge, UK) were added, and the membrane was incubated overnight at 4°C. After the membrane was washed with tris-buffered saline with tween 20 (TBST) buffer (ST671, Beyotime, Shanghai, China), HRP-conjugated secondary antibodies (1:1000, ab6721, Abcam, Cambridge, UK) were added and incubated at room temperature for 1 h. After another wash, the protein bands were detected using an enhanced chemiluminescent reagent (ECL) (P0018S, Beyotime, Shanghai, China) on a gel imaging system (ChemiDoc MP, Bio-Rad Laboratories, Hercules, California, USA). Finally, the intensities of the protein bands were quantitatively analyzed using ImageJ software (version 1.5f, National Institutes of Health, Bethesda, Maryland, USA).

Table 1: Primer sequences.

Prime name	Prime sequences (5′–3′)
ACSL4-F	CTTTTTGCGAGCTTTCCGAGTG
ACSL4-R	GAAGCCGACAATAAAGTACGCAA
GPX4-F	TCACCAAGTTTGGACACCGT
GPX4-R	ATAGTGGGGCAGGTCCTTCT
iNOS-F	CACTGCCCGGGAAATGTTTG
iNOS-R	ATGGTGACTCTGACTCGGGA
TNF-α-F	CACAGTGAAGTGCTGGCAAC
TNF-α-R	ACATTGGGTCCCCCAGGATA
Arg-1-F	ACTTAAAGAACAAGAGTGTGATGTG
Arg-1-R	GTCCACGTCTCTCAAGCCAA
IL-10-F	TGCAAAAGAAGGCATGCACAG
IL-10-R	TAGAGTCGCCACCCTGATGT
USP7-F	ATGCAGAGATGGCTGGGAAC
USP7-R	CTCAGGGCCACATTCCCATT
β-Actin-F	ACACTGTGCCCATCTACG
β-Actin-R	TGTCACGCACGATTTCC

ACSL4: Acyl-CoA synthetase long-chain family member 4, GPX4: Glutathione peroxidase 4, iNOS: Inducible nitric oxide synthase, TNF-α: Tumor necrosis factor-α, Arg-1: Arginase-1, IL-10: Interleukin-10, USP-7: Ubiquitin-specific protease 7, A: Adenine, C: Cytosine, G: Guanine, T: Thymine.

Spectrophotometric method

A malondialdehyde (MDA) assay kit was obtained, and cell samples were diluted before they were transferred to reaction tubes. After thiobarbituric acid reagent was added, the mixture was thoroughly mixed, heated in a 100°C water bath for 30 min, and allowed to cool to room temperature. After centrifugation or removal of any precipitate, absorbance was measured at 532 nm. A standard curve was used in determining MDA concentration.

A glutathione (GSH) assay kit was used for GSH detection. Samples were diluted and placed in designated wells, and 5,5′-dithiobis(2-nitrobenzoic acid) reagent was added. The cells were incubated at room temperature for 30 min, absorbance was measured at 412 nm, and GSH concentration was calculated using a standard curve.

MDA (S0131M) and GSH (S0057S) assay kits were purchased from Beyotime (Shanghai, China). A Cary 60 ultraviolet–vis spectrophotometer (Agilent Technologies, Santa Clara, California, USA) was used.

Colony formation assay

First, SKOV-3 cells were cultured in an appropriate medium until they reached the logarithmic growth phase, counted, and adjusted to 1×10^3 cells/mL. Next, a certain number of cells (1000 cells) were evenly plated in culture dishes and incubated in an incubator (Heracell Vios 160i, Thermo Fisher Scientific, Waltham, Massachusetts, USA) with 5% CO_2 at 37°C for 1 week until visible colonies formed. Subsequently, the cells were fixed with 4% formaldehyde for 10 min. The fixed cells were washed with phosphate-buffered saline (PBS) to remove the fixative and stained with crystal violet solution (G1062, Solarbio, Beijing, China) for 30 min. Unbound dye was removed by gently washing the cells. Finally, colonies formed in each well were observed and counted using an inverted microscope (IX73, Olympus Corporation, Tokyo, Japan).

Terminal deoxynucleotidyl transferase dUTP nick end labeling (TUNEL) staining

First, cells were cultured in a dish until they reached an appropriate density and then washed with PBS to remove the culture medium. Next, 4% paraformaldehyde (P0099, Beyotime, Shanghai, China) was used to fix the cells at room temperature for 20 min, and then the cells were washed with PBS 3 times. The cells were then permeabilized on ice with 0.1% Triton X-100 (P0096, Beyotime, Shanghai, China) for 10 min and again washed 3 times with PBS. Subsequently, the TUNEL reaction mixture was prepared according to the instructions of the kit (C1086, Beyotime, Shanghai, China). The mixture included terminal deoxynucleotidyl transferase and labeled dUTP. The reaction mixture was added to the cells and incubated at 37°C for 1 h in the dark. Afterward, the unbound reaction mixture was removed by gently washing the cells 3 times with PBS. After 4′,6-diamidino-2-phenylindole (DAPI; C1002, Beyotime, Shanghai, China) nuclear stain was added, and the cells were incubated for 10 min. Finally, the cells were observed using a fluorescence microscope (BX53, Olympus, Tokyo, Japan), and TUNEL-positive cells were recorded.

Reactive oxygen species (ROS) fluorescence staining

First, cells were cultured in a dish until they reached an appropriate density, and then the culture medium was removed through washing with PBS. Next, a 2′,7′-dichlorodihydrofluorescein diacetate probe solution was prepared according to the instructions of the kit (S0035S, Beyotime, Shanghai, China). The diluted ROS probe was then added to a cell culture medium. The cells were completely immersed in the staining solution and incubated at 37°C for 30 min. After incubation, the cells were gently washed 3 times with PBS for the removal of unbound probes. Next, DAPI (C1002, Beyotime, Shanghai, China) nuclear stain was added, and the cells were incubated for 10–15 min to stain the cell nuclei and then washed with PBS for the removal of unbound dye. Finally, the cells were observed using a fluorescence microscope (BX53, Beyotime, Shanghai, China), fluorescence intensity and ROS distribution were recorded, and nuclear staining was assessed.

Flow cytometry

First, cells were cultured in a dish until they reached an appropriate density, collected, and washed with PBS for the removal of the culture medium. Next, cell concentration was determined using a cell counting chamber and was set at 1×10^6 cells/mL. Then, primary antibodies against PE anti-cluster of differentiation 86 (CD86) antibody (1:1000, ab77226, Abcam, Cambridge, UK) and APC anti-cluster of differentiation 206 CD206 (1:1000, 321109, Biolegend, San Diego, California, USA) were diluted according to the instructions and added to the cell suspension. The resulting suspension was gently mixed and incubated at 4°C in the dark for 30 min. After incubation, the cells were gently washed 3 times with PBS to remove unbound antibodies. A fluorescently labeled secondary antibody (1:1000, ab6717, Abcam, Cambridge, UK) was added and incubated according to the instructions. When needed, the cells were fixed with 4% paraformaldehyde and washed with PBS afterward. Finally, the stained cells were resuspended in PBS, and the cell concentration was adjusted to 1×10^6 cells/mL, which was suitable for analysis through flow cytometry (BD LSRFortessa, BD Biosciences, Lake Franklin, New Jersey, USA). The samples were analyzed, and the fluorescence signals of CD86 and CD206 were recorded.

Statistical analysis

Data analysis was conducted using GraphPad Prism software (version 9.0, GraphPad Software, Inc., San Diego, California, USA), and the results were expressed as mean ± standard deviation. A *t*-test was utilized for comparisons between two groups, whereas a one-way analysis of variance was employed for multiple-group comparisons, followed by Tukey's *post hoc* test. $P < 0.05$ was deemed statistically significant.

RESULTS

ACSL4 inhibited EOC cell proliferation and induced ferroptosis

First, we assessed the expression of ACSL4 in ovarian epithelial cells (IOSE-80) and EOC cells (SKOV-3) through qRT-PCR and Western blot analysis. The results in Figure 1a-c indicate that the mRNA and protein levels of ACSL4 in IOSE-80 cells were significantly higher than those in SKOV-3 cells ($P < 0.001$). To further clarify the role of ferroptosis in the pathogenesis of EOC, we stimulated SKOV-3 cells with ACSL4 recombinant protein. The colony formation assay results showed that ACSL4 treatment significantly reduced the number of colonies formed by SKOV-3 cells ($P < 0.001$) [Figure 1d and e]. TUNEL staining results indicated that ACSL4 treatment significantly increased the number of apoptotic SKOV-3 cells ($P < 0.001$) [Figure 1f and g].

In addition, ROS fluorescence staining demonstrated a significant increase in ROS fluorescence intensity in SKOV-3 cells treated with ACSL4 ($P < 0.001$) [Figure 2a and b]. Compared with the control group, ACSL4 treatment elevated the levels of MDA while decreasing the levels of GSH and glutathione peroxidase 4 (GPX4) in the EOC cells ($P < 0.001$) [Figure 2c-e]. These results suggested that ACSL4 recombinant protein induces ferroptosis in EOC cells.

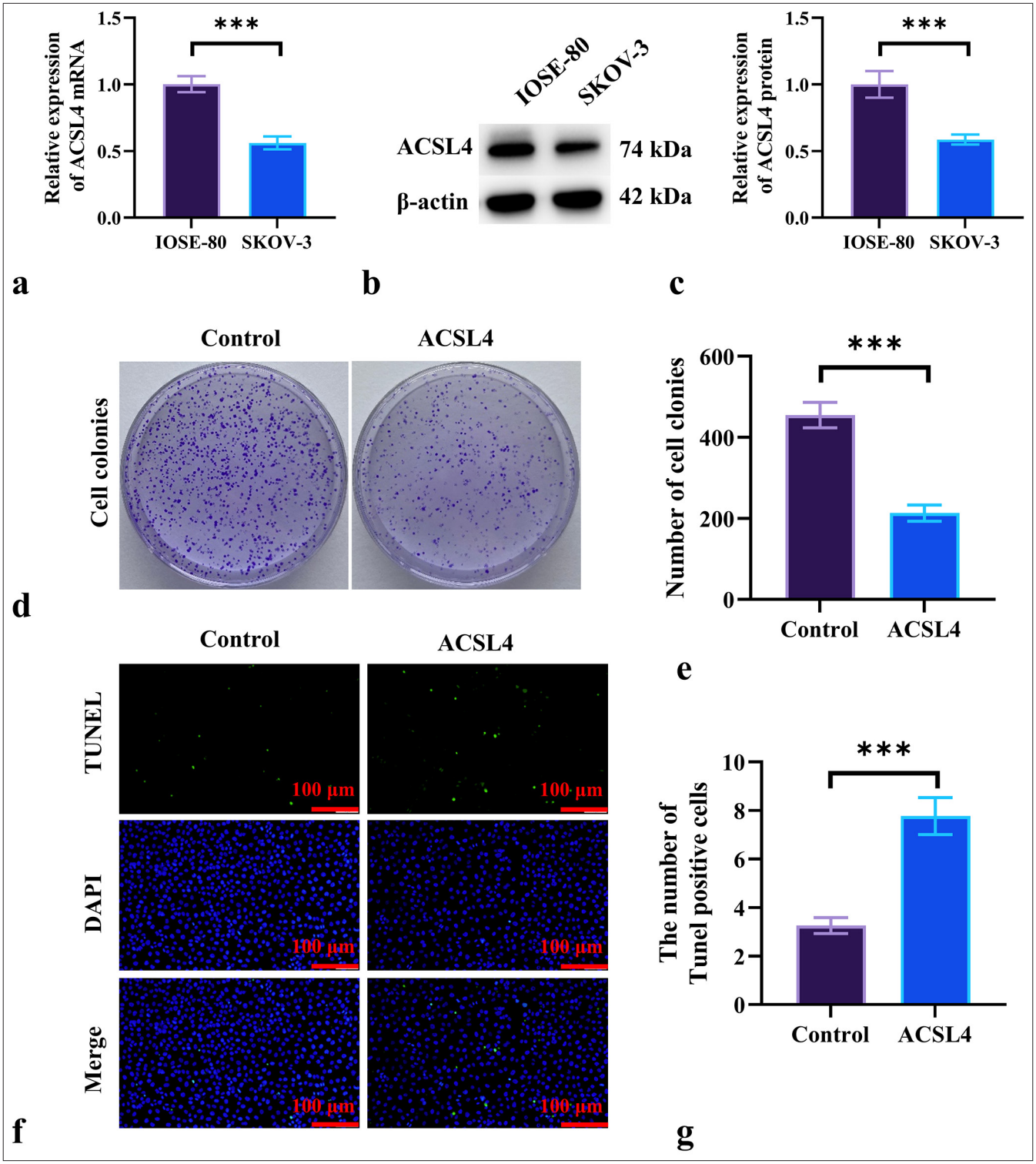

Figure 1: ACSL4 inhibits EOC cell proliferation. (a-c) mRNA and protein levels of ACSL4 in ovarian epithelial cells (IOSE-80) and EOC cells (SKOV-3) were detected by qRT-PCR and Western blot. (d and e) The assessed effect of ACSL4 recombinant protein on colony formation in SKOV-3 cells. (f and g) The effect of ACSL4 recombinant protein on apoptosis in SKOV-3 cells was measured by TUNEL staining. Magnification 200×. $n = 6$. ***$P < 0.001$. ACSL4: Acyl-CoA synthetase long-chain family member 4, TUNEL: Terminal deoxynucleotidyl transferase dUTP nick end labeling, DAPI: 4′,6-diamidino-2-phenylindole, qRT-PCR: quantitative reverse transcription polymerase chain reaction, EOC: Epithelial ovarian cancer.

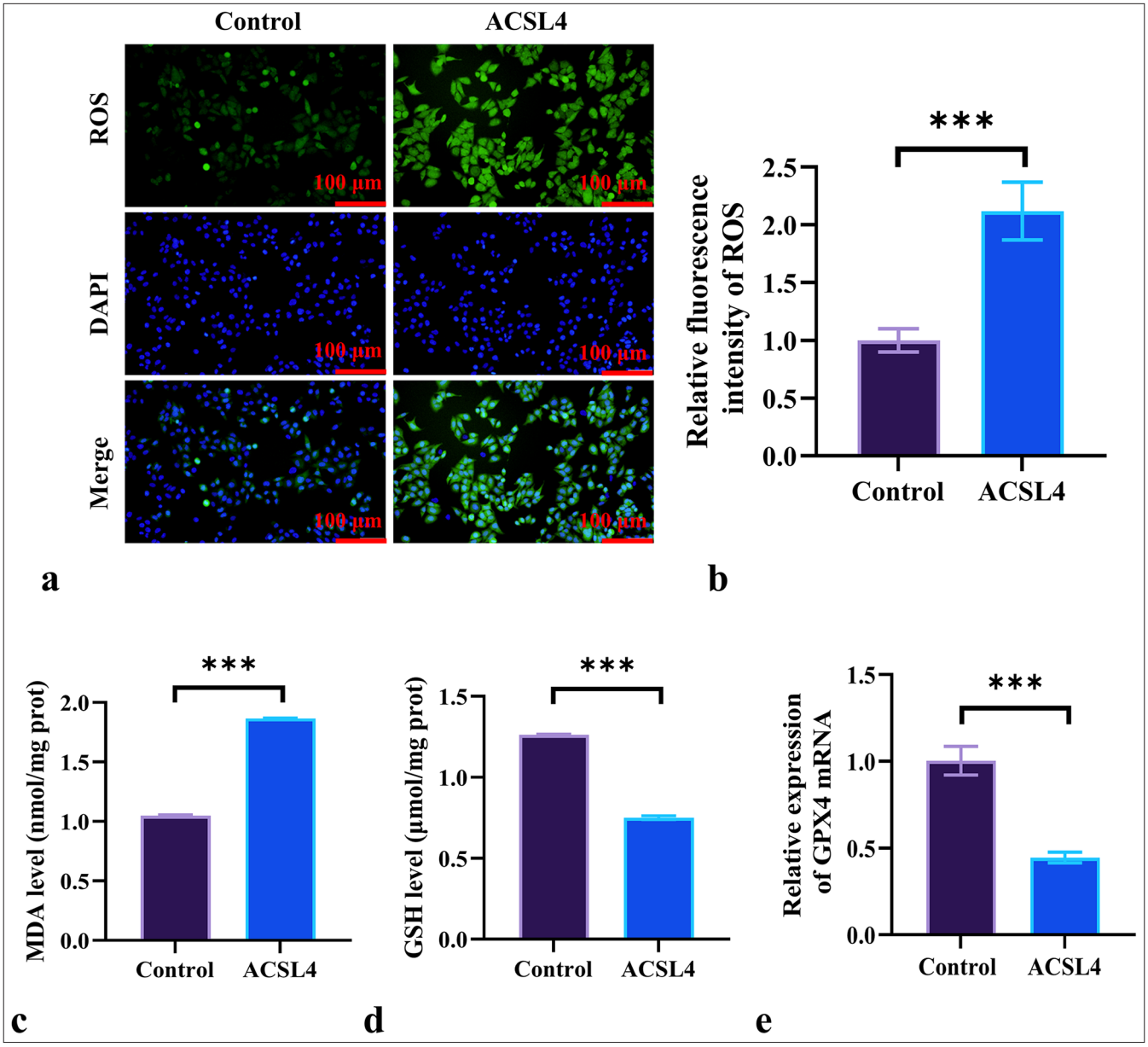

Figure 2: ACSL4 induces ferroptosis in EOC Cells. (a and b) Assessment of the effect of ACSL4 on ROS levels in SKOV-3 cells by ROS staining. Magnification 200×. (c and d) Measurement of MDA and GSH levels in SKOV-3 cells following ACSL4 treatment by spectrophotometric method. (e) Detection of the effect of ACSL4 on the mRNA expression level of GPX4 in SKOV-3 cells according to qRT-PCR. $n = 6$. ***$P < 0.001$. ROS: Reactive oxygen species, MDA: Malondialdehyde, GSH: Glutathione, GPX4: Glutathione peroxidase 4, qRT-PCR: quantitative reverse transcription polymerase chain reaction, EOC: Epithelial ovarian cancer.

ACSL4 promoted the M1 polarization of macrophages

We further investigated the effect of ACSL4 recombinant protein on macrophage polarization. SKOV-3 cells treated with ACSL4 were co-cultured with THP-1 cells. A change in CD86/CD206 ratio served as an indicator of the transition between the M1 and M2 macrophages. The results in Figures 3a and b show that the CD86/CD206 ratio was significantly higher in the THP-1/EOC (ACSL4)-CM group than in the THP-1/EOC-CM group ($P < 0.001$). The mRNA levels of the M1 markers inducible nitric oxide synthase (iNOS) and tumor necrosis factor-α (TNF-α) in the THP-1/EOC (ACSL4)-CM group were significantly elevated relative to those in the THP-1/EOC-CM group ($P < 0.001$) [Figure 3c and d]. By contrast, the mRNA expression levels of the M2 markers arginase-1 (Arg-1) and interleukin-10 (IL-10) were significantly reduced in the THP-1/EOC(ACSL4)-CM group compared with the

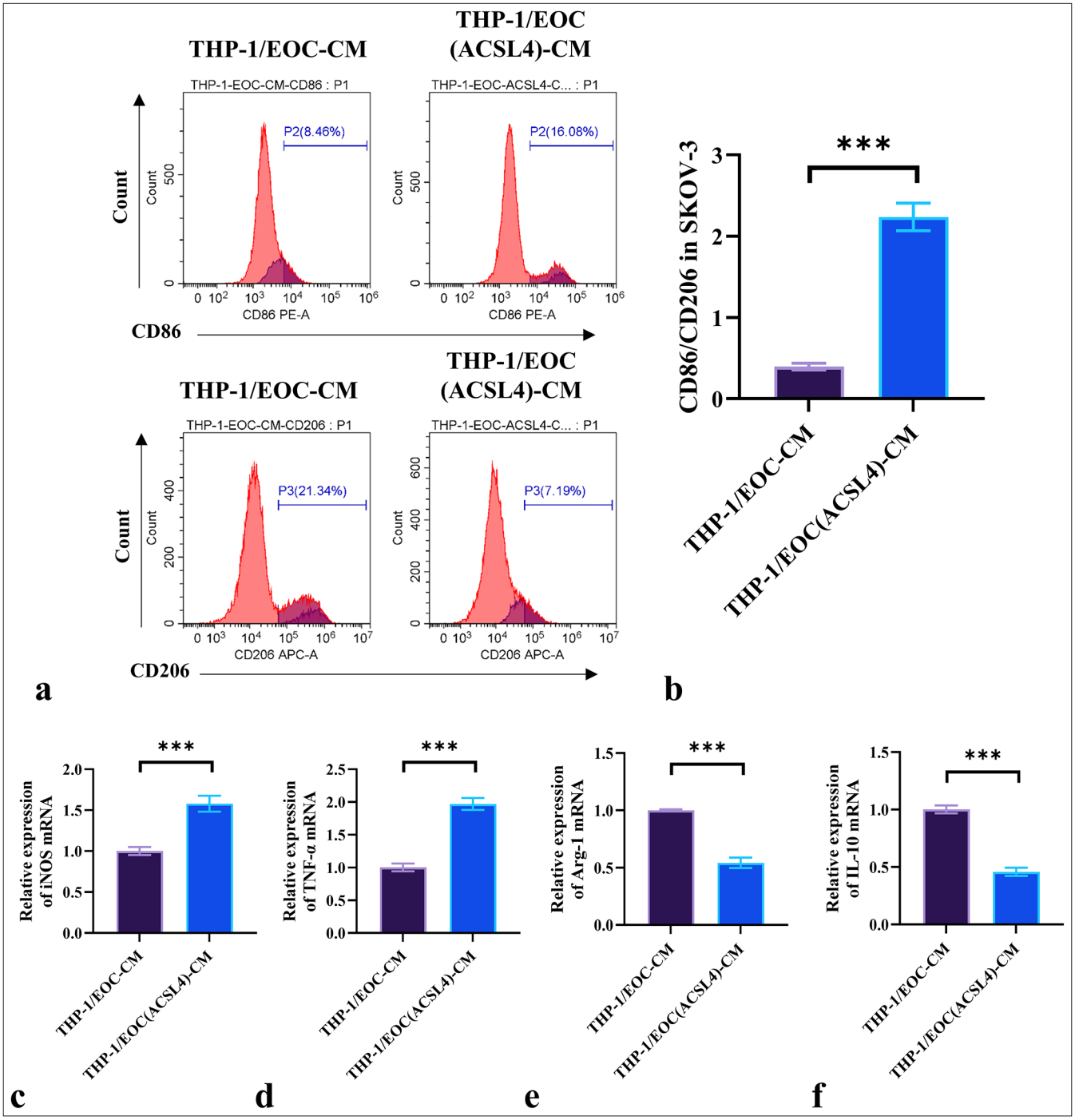

Figure 3: ACSL4 promotes the M1 polarization of macrophages. (a) THP-1 macrophages were treated with conditioned media from differently treated SKOV-3 cells, and the expression levels of CD86 and CD206 were measured by flow cytometry. (b) CD86/CD206 ratio. (c-f) THP-1 macrophages were treated with conditioned media from differently treated SKOV-3 cells, and the mRNA levels of iNOS, TNF-α, Arg-1, and IL-10 were measured by qRT-PCR. $n = 6$. ***$P < 0.001$. EOC: Epithelial ovarian cancer, THP-1/EOC-CM: THP-1 cells treated with EOC cell culture medium, THP-1/EOC (ACSL4)-CM: THP-1 cells treated with EOC cell culture medium pretreated with ACSL4, CD86: Cluster of differentiation 86, CD206: Cluster of differentiation 206, iNOS: Inducible nitric oxide synthase, TNF-α: Tumor necrosis factor-α, Arg-1: Arginase-1, IL-10: Interleukin-10, qRT-PCR: quantitative reverse transcription polymerase chain reaction, EOC: Epithelial ovarian cancer.

THP-1/EOC-CM group ($P < 0.001$) [Figure 3e-f]. These results suggested that ACSL4 regulates the pathological process of EOC by promoting the M1 polarization of macrophages.

ACSL4 counteracts the proliferation and ferroptosis resistance induced by USP7 overexpression in EOC cells

To further investigate whether USP7 mediates the regulation of ferroptosis in EOC by ACSL4, we measured the mRNA levels of USP7 in IOSE-80 and SKOV-3 cells through qRT-PCR. The results in Figure 4a show that the mRNA level of USP7 was significantly higher in the SKOV-3 cells than in the IOSE-80 cells ($P < 0.001$). We transfected SKOV-3 cells with a USP7 overexpression vector and treated them with ACSL4 recombinant protein. Figure 4b indicates that the mRNA level of USP7 was significantly elevated in the Ov-USP7 group compared with the Ov-NC group ($P < 0.001$), whereas the mRNA level in the Ov-USP7+ACSL4 group was significantly lower than that in the Ov-USP7 group ($P < 0.001$). In addition, Figure 4c demonstrates that USP7 overexpression significantly decreased the mRNA expression level of ACSL4 in SKOV-3 cells ($P < 0.001$), and the addition of ACSL4 recombinant protein markedly increased the mRNA level of ACSL4 ($P < 0.001$).

The colony formation assay results [Figure 4d and e] showed that USP7 overexpression significantly increased the number of colonies formed by SKOV-3 cells ($P < 0.001$). By contrast, the Ov-USP7+ACSL4 group displayed a significant reduction in colony formation compared with the Ov-USP7 group ($P < 0.001$). TUNEL staining results [Figure 4f and g] revealed that USP7 treatment significantly reduced the number of apoptotic SKOV-3 cells compared to the Ov-NC group ($P < 0.001$), while the addition of ACSL4 markedly increased the number of apoptotic cells ($P < 0.001$).

ROS fluorescence staining showed that the fluorescence intensity of ROS in SKOV-3 cells treated with Ov-USP7 was significantly lower than that in the Ov-NC group, and the addition of ACSL4 significantly increased the ROS fluorescence intensity compared to the Ov-USP7 group ($P < 0.001$) [Figure 5a and b]. Moreover, compared to the NC group, Ov-USP7 decreased the level of MDA ($P < 0.001$) and increased the levels of GSH and GPX4 expression ($P < 0.001$), while the addition of ACSL4 recombinant protein reversed this trend [Figure 5c-e]. ACSL4 increased the levels of MDA ($P < 0.001$) and decreased the expression levels of GSH and GPX4 ($P < 0.001$) [Figure 5c-e]. These results suggested that ACSL4 can reverse proliferation and ferroptosis resistance induced by USP7 overexpression in EOC cells.

ACSL4 reverses USP7-induced resistance to M1 macrophage polarization

We investigated whether ACSL4 mediates USP7-induced resistance M1 polarization in macrophages. The results in Figures 6a and b show that compared with the THP-1/EOC (Ov-NC)-CM group, the THP-1/EOC (Ov-USP7)-CM group exhibited a significant reduction in CD86/CD206 ratio ($P < 0.001$). Conversely, the addition of ACSL4 significantly increased the CD86/CD206 ratio in the THP-1/EOC (Ov-USP7)-CM group ($P < 0.001$). Furthermore, the results in Figures 6c-f indicate that compared with the THP-1/EOC (Ov-NC)-CM group, the THP-1/EOC (Ov-USP7)-CM group showed significantly lower mRNA levels of iNOS and TNF-α, whereas the mRNA levels of Arg-1 and IL-10 were significantly elevated ($P < 0.001$). The addition of ACSL4 reversed the effects of Ov-USP7 on iNOS, TNF-α, Arg-1, and IL-10 levels ($P < 0.001$) [Figure 6c-f]. These results suggested that ACSL4 reverses USP7-induced resistance M1 polarization in macrophages, thereby promoting M2 polarization.

DISCUSSION

In this study, we revealed the role of ACSL4 in EOC, exploring its functions in ferroptosis and macrophage polarization. We then identified the critical role of USP7 in the regulation of these processes, especially its role in reversing ACSL4-induced ferroptosis and M1 macrophage polarization. These findings not only deepen our understanding of the functional mechanisms underlying EOC progression but also provide potential research directions for future targeted therapies.

Our study demonstrated that ACSL4 can significantly induce ferroptosis in EOC, and the mechanism is consistent with ACSL4's role in other types of cancer. Previous research has shown that ACSL4 promotes the esterification of PUFAs, leading to lipid peroxidation and subsequently inducing ferroptosis in various cancer types, including glioma and pancreatic cancer.[18,19] Our experimental results showed that treatment with ACSL4 significantly increased ROS and MDA levels while decreasing GSH and GPX4 levels, indicating that ACSL4 promotes lipid peroxidation and ferroptosis by regulating antioxidant mechanisms.

However, the expression level of ACSL4 in normal epithelial cells (IOSE-80) was significantly higher than that in cancer cells (SKOV-3). This finding is consistent with reports showing that ACSL4 is highly expressed in colorectal cancer,[20] indicating that ACSL4 plays an important physiological role in the normal functions of ovarian epithelial cells. Future research can further explore the distinct regulatory functions of ACSL4 in normal versus cancer cells to better understand its role in cancer.

We also found that ACSL4 not only directly suppresses tumor progression by inducing ferroptosis in EOC cells but also further affects the tumor immune microenvironment by regulating macrophage polarization. M1 macrophage polarization exerts antitumor effects, whereas M2 polarization promotes tumor growth and metastasis.[21,22] In the present study, ACSL4-treated EOC cells significantly enhanced M1 macrophage polarization, as evidenced by a

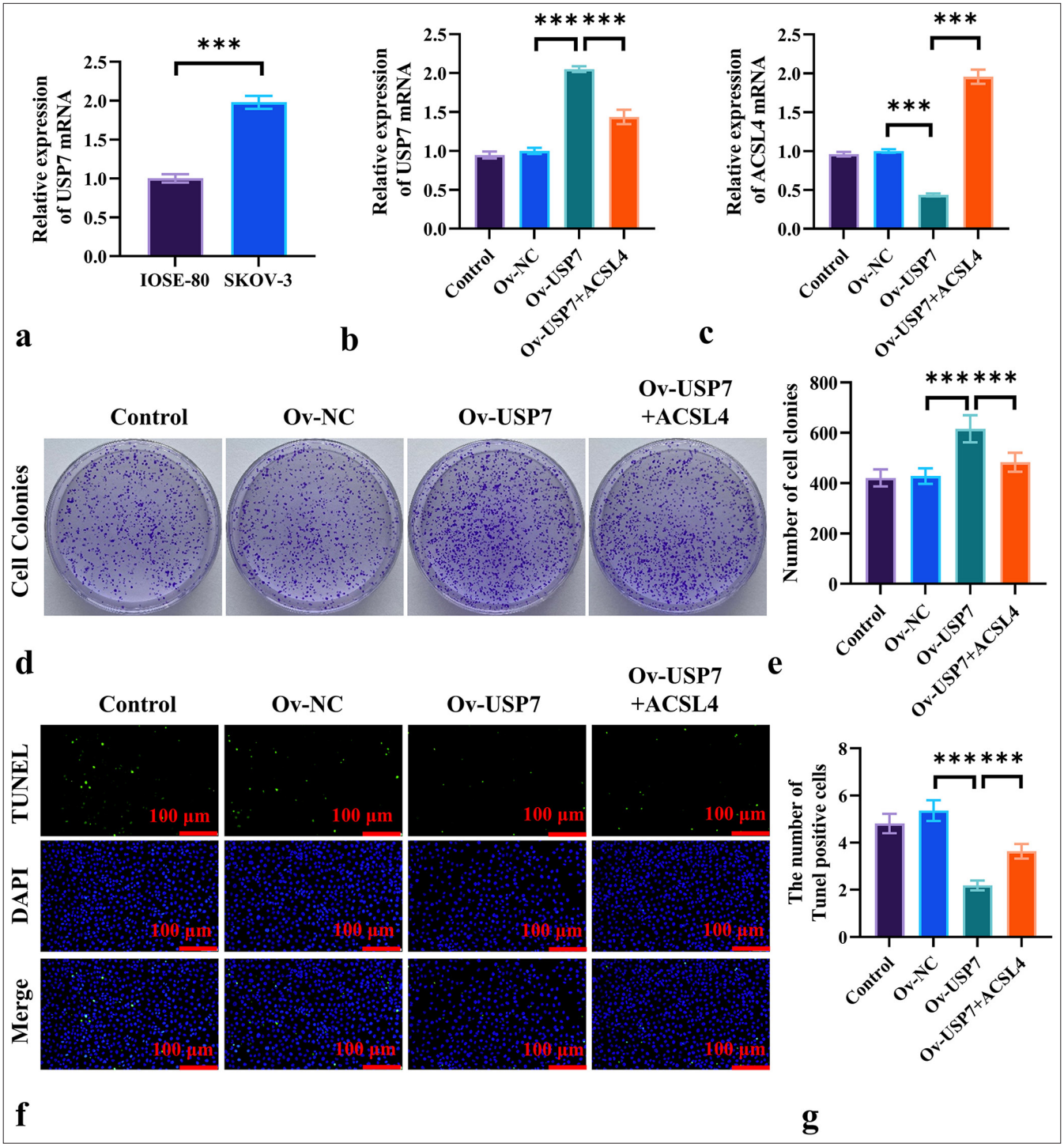

Figure 4: ACSL4 Reverses USP7-Induced Proliferation in EOC Cells. (a) The mRNA levels of USP7 in ovarian epithelial cells (IOSE-80) and EOC cells (SKOV-3) were measured by qRT-PCR. (b) The transfection of SKOV-3 cells with USP7 overexpression vector and treatment with ACSL4 recombinant protein, showing the mRNA levels of USP7 in the SKOV-3 cells. (c) The mRNA levels of ACSL4 in the SKOV-3 cells was detected by qRT-PCR. (d and e) The assessed effects of ACSL4 and USP7 on colony formation in the SKOV-3 cells. (f and g) The effects of ACSL4 and USP7 on apoptosis in the SKOV-3 cells were measured by TUNEL staining. Magnification 200×. $n = 6$. ***$P < 0.001$. USP7: Ubiquitin-specific protease 7, Ov-NC: Overexpression-negative control, Ov-USP-7: Overexpression-USP7, qRT-PCR: quantitative reverse transcription polymerase chain reaction, EOC: Epithelial ovarian cancer.

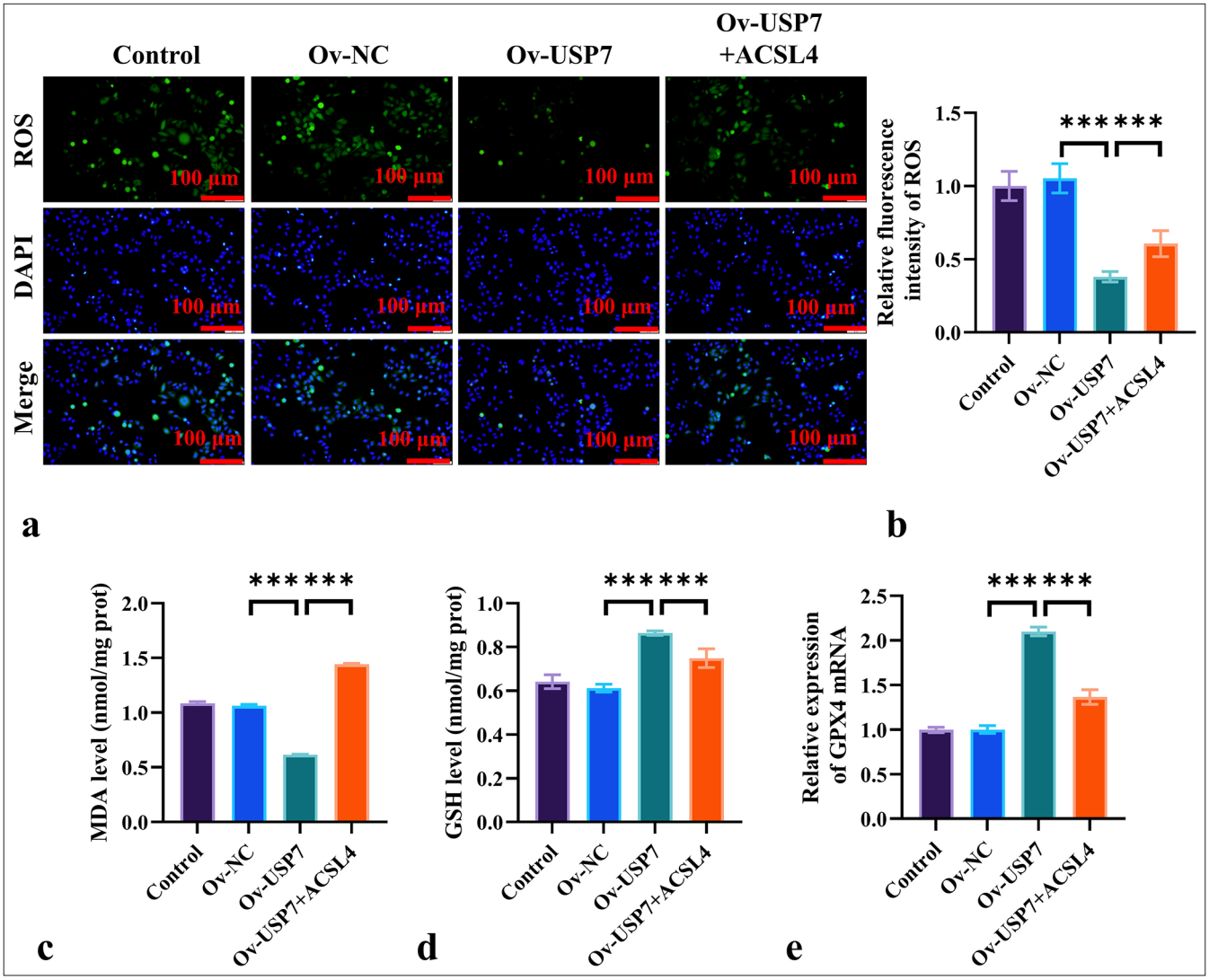

Figure 5: ACSL4 Reverses USP7-Induced Ferroptosis Resistance in EOC Cells. (a and b) Assessment of the effects of ACSL4 and USP7 on ROS levels in the SKOV-3 cells by ROS staining, magnification 200×. (c and d) The measurement of MDA and GSH levels in the SKOV-3 cells treated with ACSL4 and USP7 through ELISA. (e) The evaluation of the effects of ACSL4 and USP7 on the mRNA expression levels of GPX4 in SKOV-3 cells through qRT-PCR. Magnification 200×. $n = 6$. ***$P < 0.001$. qRT-PCR: Quantitative reverse transcription polymerase chain reaction, EOC: Epithelial ovarian cancer.

notable increase in the CD86/CD206 ratio and upregulation of iNOS and TNF-α. This result aligns with other studies regarding the role of ACSL4 in immune regulation, indicating that ACSL4 influences EOC progression not only by modulating the physiological processes of tumor cells but also by affecting immune cells within the tumor microenvironment.[23]

This finding contradicts the findings of previous studies on ACSL4 in other cancer types. For instance, Li *et al.* focused on ACSL4's role in the regulation of ferroptosis within tumor cells, whereas this study is the first to reveal ACSL4's role in the tumor microenvironment through the modulation of macrophage polarization.[24] This new discovery suggests that ACSL4 plays an important role in EOC development through a dual mechanism: directly inducing ferroptosis in tumor cells and indirectly regulating the immune microenvironment. This finding provides a novel perspective for future ACSL4-targeting therapies not only for directly suppressing tumor cells but also for enhancing immune responses within the tumor microenvironment.

Our study is the first to reveal the USP7's effect that reverses ACSL4-mediated ferroptosis and macrophage polarization in EOC. USP7 is considered a pro-cancer factor in various types of cancer, stabilizing key oncogenic proteins, such as p53 and MDM2, through its deubiquitination activity.[25] Our experimental results

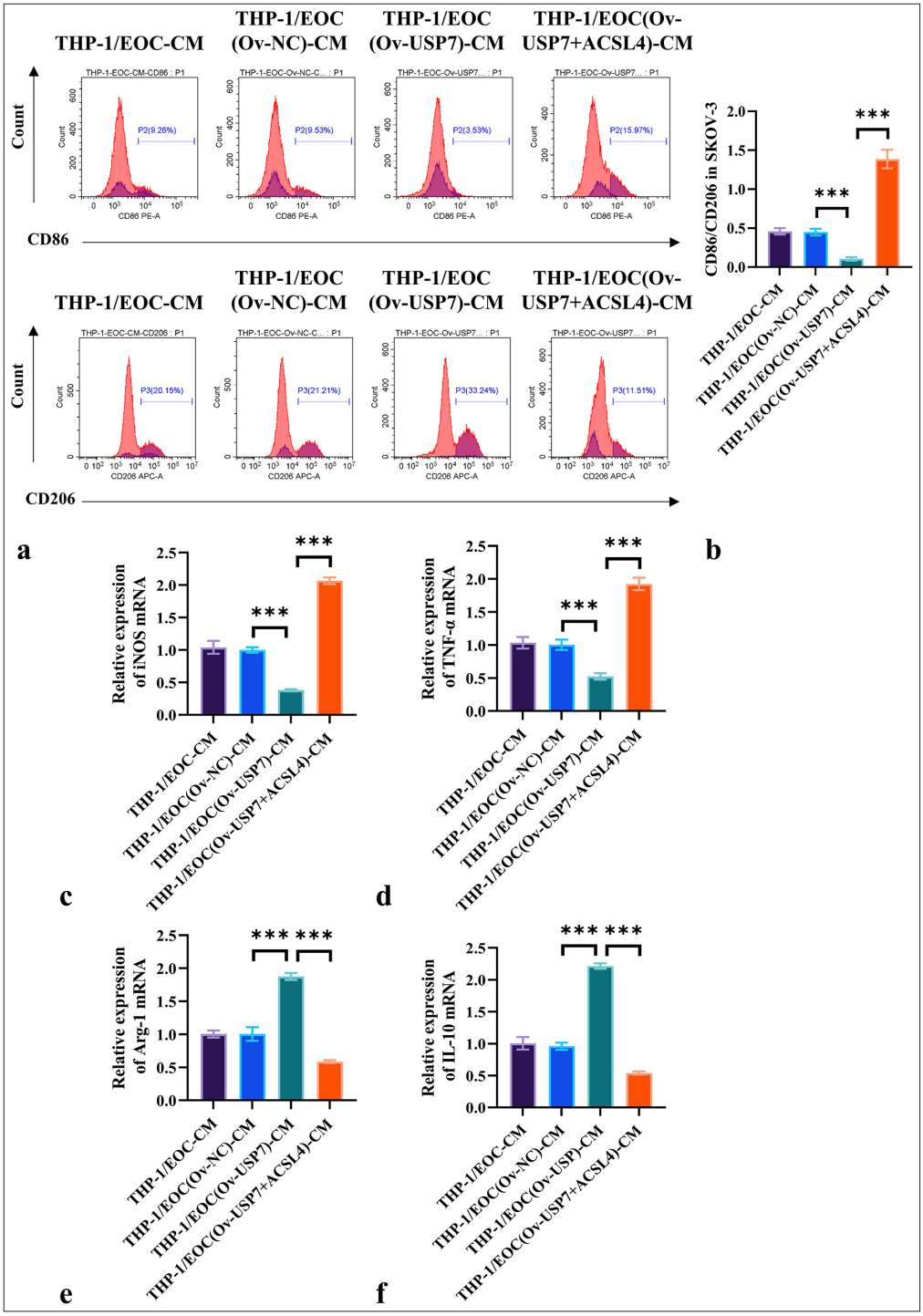

Figure 6: ACSL4 reverses USP7-induced resistance to M1 macrophage polarization. (a and b) USP7 was overexpressed in the SKOV-3 cells with or without the addition of ACSL4 recombinant protein for treatment. The THP-1 macrophages were treated with conditioned media from differently treated SKOV-3 cells, and flow cytometry was used in measuring the expression levels of CD86 and CD206. (c-f) THP-1 macrophages were treated with conditioned media from differently treated SKOV-3 cells, and the mRNA levels of iNOS, TNF-α, Arg-1, and IL-10 were assessed through qRT-PCR. $n = 6$. ***$P < 0.001$. THP-1/EOC(Ov-NC)-CM group: THP-1 cells treated with EOC cell culture medium pretreated with Ov-NC, THP-1/EOC(Ov-USP7)-CM group: THP-1 cells treated with EOC cell culture medium pretreated with Ov-USP7, THP-1/EOC(Ov-USP7+ACSL4)-CM group: THP-1 cells treated with EOC cell culture medium pretreated with Ov-USP7 and ACSL4, qRT-PCR: Quantitative reverse transcription polymerase chain reaction, EOC: Epithelial ovarian cancer.

demonstrated that USP7 overexpression considerably inhibits ferroptosis in EOC cells by elevating the levels of antioxidants, including GSH and GPX4. However, the introduction of ACSL4 effectively reversed the suppressive effect of USP7 overexpression on ferroptosis. In addition, USP7 enhanced tumor-promoting M2 polarization by inhibiting the M1 polarization of macrophages.

Our study further expanded the role of USP7, showing that it not only inhibits tumor cell death through deubiquitination mechanisms but also promotes tumor progression by regulating the immune microenvironment. This makes USP7 an attractive target for EOC treatment, as inhibiting USP7 could potentially reverse the effects of ACSL4 on ferroptosis and immune regulation, thereby inhibiting the progression of EOC.

Based on these findings, future research can further explore the molecular mechanisms of interaction between ACSL4 and USP7 in EOC, particularly regarding ferroptosis and immune regulation. By investigating the regulatory networks of ACSL4 and USP7 in-depth, novel targets may be identified, and more precise anticancer therapies can be developed.

Although this study revealed the critical roles of USP7 and ACSL4 in EOC, it has several limitations. First, the limited number of EOC cell lines used may not fully represent the heterogeneity of EOC, possibly restricting the generalizability of the results. Second, the study primarily relied on *in vitro* experiments, lacking validation in the complex tumor microenvironment *in vivo*. The absence of clinical samples further limited the assessment of USP7 and ACSL4 expression levels and their clinical relevance. In addition, the experiments were performed at specific time points, and dynamic analysis of ferroptosis and macrophage polarization over time is lacking. Future research should include a broader range of EOC cell lines and patient-derived primary cells to validate these findings, along with *in vivo* animal model studies, to investigate the role of USP7 and ACSL4 in the tumor microenvironment. Clinical sample validation is essential to explore the relationship between their expression and patient prognosis, as well as their potential as therapeutic targets. Expanding mechanistic studies and exploring targeted therapeutic strategies will help to further expand our understanding of the multifaceted roles of USP7 and ACSL4 in EOC and provide novel treatment approaches to improve patient outcomes.

SUMMARY

Overall, our study indicates that USP7 promotes the progression of EOC by inducing ferroptosis and promoting the M1 polarization of macrophages, whereas ACSL4 exerts a pro-cancer effect in EOC by reversing these actions. These findings provide important insights for novel targeted therapies for EOC treatment, offering novel perspectives for investigating the functions of ACSL4 and USP7 in cancer.

AVAILABILITY OF DATA AND MATERIALS

The data and materials that support the findings of this study are available from the corresponding author on reasonable request.

ABBREVIATIONS

ACSL4: Acyl-CoA synthetase long-chain family member 4
Arg-1: Arginase-1
CD206: Cluster of differentiation 206
CD86: Cluster of differentiation 86
DAPI: 4′,6-diamidino-2-phenylindole
EOC: Epithelial ovarian cancer
GPX4: Glutathione peroxidase 4
GSH: Glutathione
IL-10: Interleukin-10
iNOS: Inducible nitric oxide synthase
MDA: Malondialdehyde
Ov-NC: Overexpression-negative control
Ov-USP-7: Overexpression-USP7
ROS: Reactive oxygen species
THP-1/EOC (ACSL4)-CM: THP-1 cells treated with EOC cell culture medium pretreated with ACSL4
THP-1/EOC (Ov-NC)-CM group: THP-1 cells treated with EOC cell culture medium pretreated with Ov-NC
THP-1/EOC (Ov-USP7)-CM group: THP-1 cells treated with EOC cell culture medium pretreated with Ov-USP7
THP-1/EOC (Ov-USP7+ACSL4)-CM group: THP-1 cells treated with EOC cell culture medium pretreated with Ov-USP7 and ACSL4.
THP-1/EOC-CM: THP-1 cells treated with EOC cell culture medium
TNF-α: Tumor necrosis factor-α
TUNEL: Terminal deoxynucleotidyl transferase dUTP nick end labeling
USP7: Ubiquitin-specific protease 7

AUTHOR CONTRIBUTIONS

QYZ, LQW, and LGY: Conceived and designed the study; QYZ, LQW, and NJR: Responsible for data acquisition; QYZ, LQW, and CLM: Analyzed and interpreted the data; QYZ, LQW, and ZSM: Responsible for experiments; QYZ, LQW, and CLM: Drafted the first version of the manuscript; QYZ, LQW, and LGY: Critically revised the manuscript.

ETHICS APPROVAL AND CONSENT TO PARTICIPATE

This study does not involve animal and human research, so ethics approval and consent to participate not required.

ACKNOWLEDGMENT

Not applicable.

FUNDING

This research was funded by Internal Fund of Affiliated Hospital of Hebei University (Study on the expression and correlation of USP7 and Ki-67 in EOC), grant No. 2022QB22.

CONFLICT OF INTEREST

The authors declare no conflict of interest.

EDITORIAL/PEER REVIEW

To ensure the integrity and highest quality of CytoJournal publications, the review process of this manuscript was conducted under a **double-blind model** (authors are blinded for reviewers and vice versa) through an automatic online system.

REFERENCES

1. Webb PM, Jordan SJ. Global epidemiology of epithelial ovarian cancer. Nat Rev Clin Oncol 2024;21:389-400.
2. Sambasivan S. Epithelial ovarian cancer: Review article. Cancer Treat Res Commun 2022;33:100629.
3. Wang CK, Chen TJ, Tan GY, Chang FP, Sridharan S, Yu CA, *et al.* MEX3A Mediates p53 degradation to suppress ferroptosis and facilitate ovarian cancer tumorigenesis. Cancer Res 2023;83:251-63.
4. Ruan D, Wen J, Fang F, Lei Y, Zhao Z, Miao Y. Ferroptosis in epithelial ovarian cancer: A burgeoning target with extraordinary therapeutic potential. Cell Death Discov 2023;9:434.
5. Zhang HL, Hu BX, Li ZL, Du T, Shan JL, Ye ZP, *et al.* PKCβII phosphorylates ACSL4 to amplify lipid peroxidation to induce ferroptosis. Nat Cell Biol 2022;24:88-98.
6. Ding K, Liu C, Li L, Yang M, Jiang N, Luo S, *et al.* Acyl-CoA synthase ACSL4: An essential target in ferroptosis and fatty acid metabolism. Chin Med J (Engl) 2023;136:2521-37.
7. Zeng K, Li W, Wang Y, Zhang Z, Zhang L, Zhang W, *et al.* Inhibition of CDK1 overcomes oxaliplatin resistance by regulating ACSL4-mediated ferroptosis in colorectal cancer. Adv Sci (Weinh) 2023;10:e2301088.
8. Yang H, Hu Y, Weng M, Liu X, Wan P, Hu Y, *et al.* Hypoxia inducible lncRNA-CBSLR modulates ferroptosis through m6A-YTHDF2-dependent modulation of CBS in gastric cancer. J Adv Res 2022;37:91-106.
9. Monaco ME. ACSL4: Biomarker, mediator and target in quadruple negative breast cancer. Oncotarget 2023;14:563-75.
10. Tang B, Zhu J, Wang Y, Chen W, Fang S, Mao W, *et al.* Targeted xCT-mediated ferroptosis and protumoral polarization of macrophages is effective against HCC and enhances the efficacy of the anti-PD-1/L1 response. Adv Sci (Weinh) 2023;10:e2203973.
11. Dai E, Han L, Liu J, Xie Y, Kroemer G, Klionsky DJ, *et al.* Autophagy-dependent ferroptosis drives tumor-associated macrophage polarization via release and uptake of oncogenic KRAS protein. Autophagy 2020;16:2069-83.
12. Yang Y, Wang Y, Guo L, Gao W, Tang TL, Yan M. Interaction between macrophages and ferroptosis. Cell Death Dis 2022;13:355.
13. Boutilier AJ, Elsawa SF. Macrophage polarization states in the tumor microenvironment. Int J Mol Sci 2021;22:6995.
14. Saha G, Roy S, Basu M, Ghosh MK. USP7 - a crucial regulator of cancer hallmarks. Biochim Biophys Acta Rev Cancer 2023;1878:188903.
15. Park HB, Baek KH. Current and future directions of USP7 interactome in cancer study. Biochim Biophys Acta Rev Cancer 2023;1878:188992.
16. Al-Eidan A, Wang Y, Skipp P, Ewing RM. The USP7 protein interaction network and its roles in tumorigenesis. Genes Dis 2022;9:41-50.
17. Le Clorennec C, Lee K, Huo Y, Zage PE. USP7 Inhibition suppresses neuroblastoma growth via induction of p53-mediated apoptosis and EZH2 and N-Myc downregulation. Int J Mol Sci 2023;24:13780.
18. Cheng J, Fan YQ, Liu BH, Zhou H, Wang JM, Chen QX. ACSL4 suppresses glioma cells proliferation via activating ferroptosis. Oncol Rep 2020;43:147-58.
19. Tao P, Jiang Y, Wang H, Gao G. CYP2J2-produced epoxyeicosatrienoic acids contribute to the ferroptosis resistance of pancreatic ductal adenocarcinoma in a PPARγ-dependent manner. Zhong Nan Da Xue Xue Bao Yi Xue Ban 2021;46:932-41.
20. Chen C, Yang Y, Guo Y, He J, Chen Z, Qiu S, *et al.* CYP1B1 inhibits ferroptosis and induces anti-PD-1 resistance by degrading ACSL4 in colorectal cancer. Cell Death Dis 2023;14:271.
21. Tang Y, Hu S, Li T, Qiu X. Tumor cells-derived exosomal circVCP promoted the progression of colorectal cancer by regulating macrophage M1/M2 polarization. Gene 2023;870:147413.
22. Meng Z, Zhang R, Wang Y, Zhu G, Jin T, Li C, *et al.* miR-200c/PAI-2 promotes the progression of triple negative breast cancer via M1/M2 polarization induction of macrophage. Int Immunopharmacol 2020;81:106028.
23. Chen P, Wang D, Xiao T, Gu W, Yang H, Yang M, *et al.* ACSL4 promotes ferroptosis and M1 macrophage polarization to regulate the tumorigenesis of nasopharyngeal carcinoma. Int Immunopharmacol 2023;122:110629.
24. Li Y, Ma Z, Li W, Xu X, Shen P, Zhang SE, *et al.* PDPN(+) CAFs

facilitate the motility of OSCC cells by inhibiting ferroptosis via transferring exosomal lncRNA FTX. Cell Death Dis 2023;14:759.
25. Oliveira RI, Guedes RA, Salvador JAR. Highlights in USP7 inhibitors for cancer treatment. Front Chem 2022;10: 1005727.

How to cite this article: Qi Y, Li Q, Chen L, Zhao S, Nie J, Liu G. A new perspective: Acyl-CoA synthetase long-chain family member 4 inhibits ubiquitin-specific protease 7-induced epithelial ovarian cancer progression by inducing ferroptosis and M1 macrophage polarization. CytoJournal. 2025;22:28. doi: 10.25259/Cytojournal_241_2024

HTML of this article is available FREE at:
https://dx.doi.org/10.25259/Cytojournal_241_2024